Temperature-Dependent Quenching Rate Constants of NF($a^1\Delta$)

Gerald C. Manke II,* Thomas L. Henshaw, Timothy J. Madden, and Gordon D. Hager

Air Force Research Laboratory, AFRL/DELC, 3550 Aberdeen Ave SE, Kirtland AFB, New Mexico 87117-5776

Received: September 28, 1999; In Final Form: December 14, 1999

The temperature dependence of the rate constants for NF($a^1\Delta$) quenching by Cl_2, HCl, O_2, and CO over the temperature range 300−480 K have been measured in a flow reactor. The rate constant data were fit by Arrhenius expressions $k(T, Cl_2) = 1.6 \pm 1.0 \times 10^{-11} \exp(-1100 \pm 250/T)$, $k(T, HCl) = 2.0 \pm 1.0 \times 10^{-10} \exp(-3270 \pm 250/T)$, $k(T, O_2) = 1.5 \pm 0.5 \times 10^{-14} \exp(-300 \pm 150/T)$ and $k(T, CO) = 2.0 \pm 1.0 \times 10^{-12} \exp(-2000 \pm 250/T)$, cm^3 $molecules^{-1}$ s^{-1}. Reaction mechanisms and possible products are discussed for each reaction.

Introduction

Since the invention of the chemical oxygen iodine laser (COIL)[1] in the late 1970s, there has been enormous interest in the chemistry of the isovalent $O_2(a^1\Delta)$,[2] $NH(a^1\Delta)$,[3−8] $NF(a^1\Delta)$,[9−14] $NBr(a^1\Delta)$,[15] and $NCl(a^1\Delta)$[16] molecules. In general, the reactivity of the ($a^1\Delta$) molecules increases in the series O_2 < NCl < NBr < NF < NH. In addition, O_2, NF, and NCl are known to have energy transfer reactions with atomic iodine, with varying degrees of efficiency. Unlike $O_2(a^1\Delta)$, which is commonly generated in the aqueous phase, the nitrenes can be generated in a completely gas-phase environment amenable to flow tube quenching rate constant measurements and potential lightweight chemical lasers. One of the most common methods for generating NF($a^1\Delta$) is the F + HN_3 reaction system,[9] which is summarized by reactions 1 and 2:

$$F + HN_3 \rightarrow HF + N_3 \quad (1)$$

$$F + N_3 \rightarrow NF(a^1\Delta) + N_2 \quad (2)$$

The reactivity of NF($a^1\Delta$) has been thoroughly characterized at room temperature by Setser and co-workers who have compiled an extensive database of molecular and atomic quenchers.[9−13] The quenching mechanism (chemical or physical) and products for a few reactions have been identified. For example, the reactions of NF($a^1\Delta$) with Cl_2 and CO have been characterized.[11,17]

$$NF(a^1\Delta) + Cl_2 \rightarrow NFCl_2^*(\tilde{X}, {}^1A') \quad (3)$$

$$NFCl_2^*(\tilde{X}, {}^1A') \rightarrow NFCl + Cl \quad (4a)$$

$$\rightarrow NCl(X^3\Sigma^-) + ClF \quad (4b)$$

$$\rightarrow NF(X^3\Sigma^-) + Cl_2 \quad (4c)$$

$$NF(a^1\Delta) + CO \rightarrow FNCO^* \rightarrow NCO(\tilde{X}^2\Pi) + F \quad (5a)$$

$$\rightarrow NF(X^3\Sigma^-) + CO \quad (5b)$$

In both cases, explicit checks for the presence of $NF(X^3\Sigma^-)$ were made, and its absence indicated that the chemical channels (4a,b, 5a) were dominant. Indeed, stoichiometric conversion of NF($a^1\Delta$) to $NCO(\tilde{X}^2\Pi)$ was observed for reaction 5. A measurement of the quenching rate constant for CO at 196 K by Du and Setser[10] is also consistent with a chemical reaction and suggests an activation energy of ∼3 kcal mol^{-1}. Presumably, reaction 4a is the dominant channel for reaction with Cl_2 since generation of $NCl(X^3\Sigma^-)$ + ClF requires traversal of a singlet−triplet curve crossing, and $NCl(a^1\Delta)$ + ClF is ∼4 kcal mol^{-1} endothermic.

The reaction with HCl is slow at room temperature and is expected to proceed via insertion to give vibrationally excited HNFCl*. Although the specific products of NF($a^1\Delta$) + HCl have not been identified, the unimolecular decomposition pathways for the intermediate species have been examined by reactions of H atoms with NFCl,[18] and $NH(a^1\Delta)$ + ClF:[19]

$$NF(a^1\Delta) + HCl \rightarrow HNFCl^* \quad (6)$$

$$H + NFCl \rightarrow HNFCl^* \quad (7)$$

$$NH(a^1\Delta) + ClF \rightarrow HNFCl^* \quad (8)$$

$$HNFCl^* \rightarrow HF + NCl(X^3\Sigma^-) \quad (9a)$$

$$\rightarrow HCl + NF(X^3\Sigma^-) \quad (9b)$$

$$\rightarrow HF + NCl(a^1\Delta) \quad (9c)$$

$$\rightarrow HCl + NF(a^1\Delta) \quad (9d)$$

$$\rightarrow Cl + HNF(X\,{}^2A'') \quad (9e)$$

The production of NF($a^1\Delta$) from H + NFCl was observed to be a major channel by both the Setser[18] and Coombe laboratories[20] even though the NF($a^1\Delta$) production channel is 30 kcal mol^{-1} less exothermic than HF + $NCl(a^1\Delta)$. The production of Cl + HNF (reaction 9e) was not considered in either of the H + NFCl experiments even though it is a viable set of products. Both NF($a^1\Delta$) and NCl($a^1\Delta$) were observed following quenching of $NH(a^1\Delta)$ by ClF,[19] and the branching ratio was ≥0.9 in favor of NF($a^1\Delta$) + HCl.

The quenching reaction of NF($a^1\Delta$) by $O_2(X^3\Sigma^-)$ is almost certainly physical. Unfortunately, the radiative lifetime of $O_2(a^1\Delta)$ precludes its observation at the low densities. While the room-temperature rate constant for reaction 9,[10]

$$NF(a^1\Delta) + O_2(X^3\Sigma^-_g) \rightarrow NF(X^3\Sigma^-) + O_2(a^1\Delta) \quad (10)$$

10.1021/jp993477+
Published on Web 02/04/2000

is $7.0 \pm 0.7 \times 10^{-15}$ cm^3 molecules^{-1} s^{-1}, estimates of efficient energy transfer between NF($a^1\Delta$) and O_2 at high temperatures have fueled speculation that a high-density source of NF($a^1\Delta$) could replace the aqueous chemistry currently used to generate gas-phase $O_2(a^1\Delta)$.[21] Electronic energy transfer reactions do not typically have a strong temperature dependence, and in fact the published nonambient rate constant measurements (k(196 K)[10] $= 2.8 \pm 0.5 \times 10^{-15}$ and k(421 K)[22] $= 8.2 \pm 0.8 \times 10^{-15}$ cm^3 molecules^{-1} s^{-1}) are consistent with the Arrhenius expression $k(T) = 3.8 \times 10^{-14} \exp(-533/T)$ and $E_a = 1.06$ kcal mol^{-1}. If this relationship holds across a wide range of temperatures, energy transfer from NF($a^1\Delta$) would not be a useful source of $O_2(a^1\Delta)$.

Other than reactions 5 and 9, there have been few temperature-dependent quenching measurements for NF($a^1\Delta$).[22] We seek to expand this list and further characterize the chemical reactivity of NF($a^1\Delta$) by measuring the temperature-dependent quenching rate constants of NF($a^1\Delta$) for Q = HCl, Cl_2, CO, and O_2 over the temperature range of 300−480 K.

Experimental Methods

The high temperature flow reactor (HTFR) used for this experiment has been described in detail previously,[23] and a few minor modifications are described below. First, an indicator inlet was installed 5 cm upstream of the observation zone to allow the addition of $N_2(A^3\Sigma^+_u)$ or H_2S. Metastable $N_2(A^3\Sigma^+_u)$ molecules were generated by energy transfer from Ar ($^3P_2$, $^3P_0$) atoms using a rolled tantalum foil discharge design.[24] Also, the quartz rods were removed and glass windows were installed. Fluorine atoms were generated with a pair of microwave discharges (typically 30 W each) on a mixture of Ar and CF_4. The initial F atom concentrations, $[F]_0$, were determined by chemiluminescent titrations. A small flow of H_2S(Matheson, CP grade) was added through the indicator inlet and the HF($\Delta v = -3$) emission at 875 nm monitored as a function of added Cl_2(3% in He, Matheson). The smoothly extrapolated, zero-intensity intercept from plots of I(HF) vs $[Cl_2]$ gives $[F]_0$.

The mechanical pump/blower combination produced linear flow velocities of 3400−1150 at 0.5−1.5 Torr when throttled with a gate valve. Absolute capacitance manometers (Baratron, model 622), measured reactor pressure, and all reagents except HCl, O_2, and CO were metered with calibrated MKS mass flow meters (Model 1179A). Quenchers O_2 (RHG grade, Spectra Gas), Cl_2 (3% in He, Matheson), and CO (UHP grade, Matheson) were loaded with or without dilution into 12 L bulbs or metered directly from the bottles without further purification. Several freeze pump-thaw-cycles were performed while preparing 15−30% mixtures of HCl (Scott Specialty Gas, 99.999%). The flow rates of HCl, CO, and O_2 were determined by diverting the stream to a vessel of known volume and measuring the rate of pressure rise. The bulk of the flow (typically 2.5 SLPM, 1850 μmol s^{-1}) consisted of Ar (Airgas, UHP grade). Two microwave discharges on a CF_4 (Airgas, 99.5%)/Ar mixture produced up to 1.5×10^{13} cm^{-3} F atoms at 1.5 Torr. Pre-prepared mixtures of HN_3 and He were stored in a stainless steel vessel, and HN_3 was added to the reactor via one of two sliding Pyrex injectors.

The entire reactor was encased by resistive heating units, which consisted of Nichrome wire helically wound inside a ceramic jacket. The temperature was measured by inserting several type K thermocouples into the gas stream at various points along the reactor. A flexible thermocouple was inserted into the one of the movable injectors to provide a temperature measurement at the center of the tube. The heaters were regulated with Omega controllers (Model CN76000) with an accuracy of ±1° at room temperature and ± 7° at 480 K. All inner surfaces were coated with PTFE, which limited the temperature to less than 500 K.

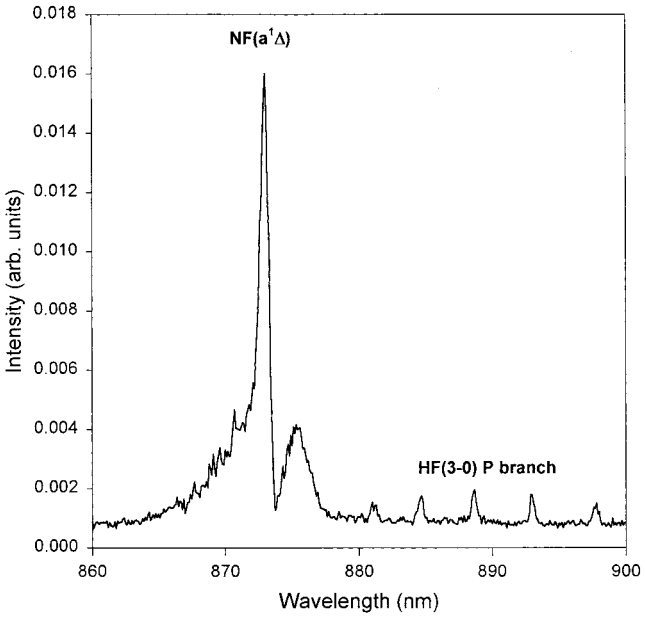

Figure 1. NF($a^1\Delta$) spectrum. The NF($a^1\Delta$) spectrum shown was measured for $[F]_0 = 1.8 \times 10^{13}$, $[HN_3]_0 = 1.2 \times 10^{13}$, and $\Delta t = 0.03$ s. Quenching measurements were normally performed with slightly lower reagent densities and $[HN_3]_0 > [F]_0$. The HF(3−0) P branch lines at 880−900 nm were not normally observable at typical quenching experimental conditions.

A 0.3 m monochromator (Instruments S.A.) dispersed the chemiluminescence collected by a short focal length lens. A grating with a 900 nm blaze and 1200 grooves/mm was used. The emissions of HF($\Delta v = -3$), NF($a^1\Delta$), and NF($b^1\Sigma^+$) were monitored with a cooled (−80 °C) R1767 PMT (Hamamatsu). When necessary, band-pass or long pass filters were used to isolate signals of interest from unwanted background or second-order emissions. A typical NF($a^1\Delta$) spectrum (uncorrected for the relative response of the S-1 PMT) from the reaction of F atoms with HN_3 is shown in Figure 1.

Observable intensities of NF($a^1\Delta$) were generated by adding HN_3 to a stream of F atoms. Conditions suitable for quenching measurements were achieved at $[F] \leq 1.0 \times 10^{13}$, and $[HN_3] = 8.0 \times 10^{12}$ cm^{-3} and $\Delta t \geq 10$ ms. Quenching reagents were added 10−40 cm downstream (10−20 ms) of the HN_3 inlet, ensuring that reactions 1 and 2 had gone to completion. The quenching rate constants were determined from plots of ln I(NF($a^1\Delta$)) vs [Quencher]. The slopes of these plots are equal to the product $k_Q\Delta t$, where Δt is the reaction time. The reaction time is calculated from the plug flow approximation, with a 5 cm (~3 ms) correction for mixing.

Each day prior to heating the reactor, several measurements of the room-temperature quenching rate constant for NF($a^1\Delta$) + Cl_2 were performed to confirm that appropriate conditions for quenching measurements existed. In all cases, the observed k_Q(NF($a^1\Delta$)) were in agreement with the established value within the combined error limits, see below. Room-temperature measurements of k_Q for Q = HCl, O_2, and CO were also consistent with the measurements of Du and Setser.[10]

Results and Discussion

The quenching data are summarized in Figures 2−7 and Tables 1 and 2. The details for individual molecules are described below:

TABLE 1: Temperature-Dependent Quenching Rate Constants for NF($a^1\Delta$)[a]

temp	$k(O_2)$	k(HCl)	$k(Cl_2)$	k(CO)
196[b]	0.28 ± 0.03	–	–	0.052 ± 0.005
300	0.62 ± 0.30 [3]	0.36 ± 0.22 [3]	49 ± 9.2 [14]	0.286 ± 0.08 [3]
	0.70 ± 0.07[b]	0.16 ± 0.03[b]	58 ± 6[b]	0.36 ± 0.04[b]
353	–	1.6 ± 0.84 [3]	–	0.65 ± 0.10 [3]
358	0.44 ± 0.28 [3]	–	73 ± 18 [3]	–
393	0.75 ± 0.47 [3]	6.6 ± 2.9 [3]	117 ± 23 [3]	1.2 ± 0.39 [3]
403	0.81 ± 0.20 [1]	–	–	–
413	0.55 ± 0.08 [3]	15.7 ± 3.1 [3]	137 ± 39 [3]	1.27 ± 0.31 [3]
421[c]	0.82 ± 0.08	–	–	–
438	0.88 ± 0.17 [1]	–	–	–
448	0.67 ± 0.20 [3]	–	–	–
453	–	–	–	2.0 ± 0.46 [3]
473	0.65 ± 0.29 [4]	28.2 ± 5.5 [3]	156 ± 21 [4]	3.3 ± 0.91 [4]
488	0.75 ± 0.10 [2]	–	184 ± 20 [4]	3.2 ± 0.20 [2]

[a] Error is 2σ, units: 10^{-14} cm^3 molecules^{-1} s^{-1}; number in brackets is number of replicate measurements. [b] Reference 10. [c] Reference 19.

TABLE 2: Arrhenius Expressions for NF($a^1\Delta$) + Q

quencher	$k(T)$[a] cm^3 molecules^{-1} s^{-1}	E_a (kcal mol^{-1})
HCl	$2.0 \pm 1.0 \times 10^{-10}$ exp(−3270 ± 250/T)	6.5 ± 0.5
Cl_2	$1.6 \pm 1.0 \times 10^{-11}$ exp(−1100 ± 250/T)	2.2 ± 0.5
CO	$2.0 \pm 1.0 \times 10^{-12}$ exp(−2000 ± 250/T)	4.0 ± 0.5
O_2	$1.5 \pm 0.5 \times 10^{-14}$ exp(−300 ± 150/T)	0.6 ± 0.3

[a] R = 1.987 cal mol^{-1} K^{-1}.

(i) Quenching by Cl_2: Molecular chlorine was used as an internal standard to verify appropriate experimental conditions. Three measurements were made each day at room temperature before heating the reactor. At all temperatures (although to a smaller degree at high T) the initial loss of NF($a^1\Delta$) upon addition of small [Cl_2] was large, but further addition of Cl_2 resulted in slower quenching, and linear plots were obtained, see Figure 2. Du and co-workers reported a similar problem and were able to eliminate the fast component by replacing the reactor. In our case, the reactor is not easily (cheaply) replaced, and the problem seemed to occur only for molecules that react with F atoms—Cl_2 and HCl (see below). This problem can be associated with backstreaming of the quenching reagent, but the fast component persisted even when [HN_3] ≫ [F], and [F] ≅ 0 far upstream of the Cl_2 injection point. Two-component quenching plots can also be attributed to a [reagent] dependent surface quenching term,[16,25] i.e., the first-order rate constant for surface quenching is a function of [Cl_2].

$$k_{\text{surface}} = f[Q]^*\frac{\text{surface}}{P} \qquad (11)$$

This surface quenching term could also be a function of temperature, which would explain why the difference between the two components decreased with increased temperature. Nonetheless, the slow component of the room-temperature data was consistent with the established rate constant,[10] k(300 K) = $5.8 \pm 0.6 \times 10^{-13}$ cm^3 molecules^{-1} s^{-1}, and we used only the slow component in determining $k(T, Cl_2)$. The quenching rate of NF($a^1\Delta$) by Cl_2 increased modestly with increased temperature. The Arrhenius plot in the lower panel of Figure 2 gives $k(T, Cl_2) = 1.6 \pm 1.0 \times 10^{-11}$ exp(−1100 ± 250/T) cm^3 molecules^{-1} s^{-1} and $E_a = 2.2 \pm 0.5$ kcal mol^{-1}.

Interestingly, NCl($a^1\Delta$) and NCl($b^1\Sigma^+$) spectra were observed for both room and high-temperature quenching of NF($a^1\Delta$) by Cl_2. Figure 3 shows the NCl($a^1\Delta$) spectrum measured at the following conditions: T = 413 K, $[HN_3]_0 = 1.3 \times 10^{13}$, $[F]_0 = 7.7 \times 10^{12}$, and $[Cl_2]_0 = 2.5 \times 10^{13}$ cm^{-3}. At the point of Cl_2 injection (Δt = 0.019 s), [F] ≈ 0, and [HN_3] = 6.4×10^{12}. The presence of HN_3 was confirmed by adding $N_2(A\ ^3\Sigma^+_u)$ and observing a NH($A\ ^3\Pi$) spectrum, while the absence of F atoms was confirmed by the absence of an HF(3−0) spectrum upon addition of H_2S 5 cm upstream of the observation zone. In addition to HN_3, a residual [N_3] ≅ 5.4×10^{12} should also be present. The observed NCl($b^1\Sigma^+$) was quite weak and is most likely generated by NCl($a^1\Delta$) energy pooling. The intensity of the NCl($a^1\Delta$) spectrum is also consistent with the branching fraction of the Cl + N_3 reaction.[26] The conversion efficiency, [NF($a^1\Delta$)]$_{\text{lost}}$: [NCl($a^1\Delta$)]$_{\text{total}}$, where [NX($a^1\Delta$)] is calculated using eq 12,

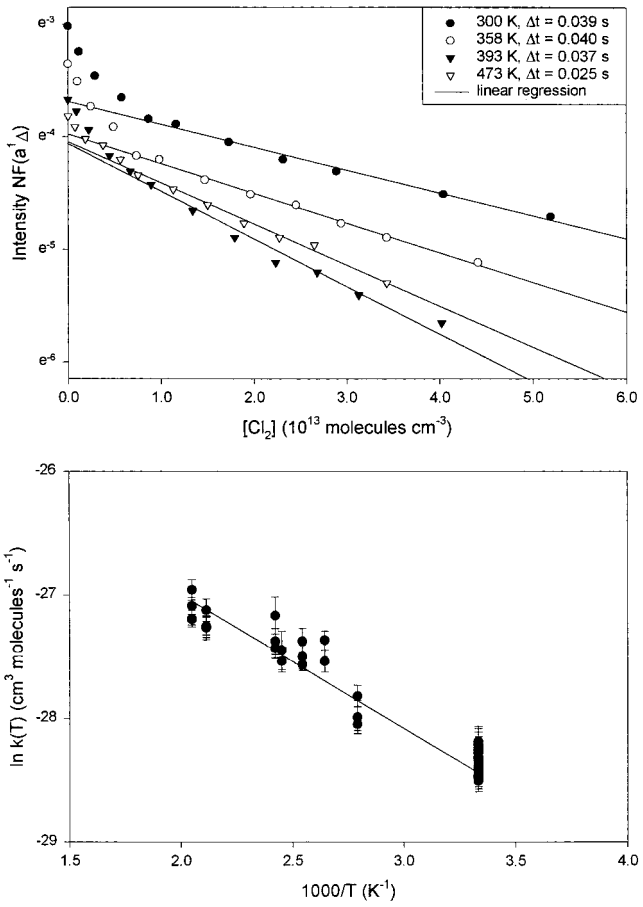

Figure 2. Temperature-dependent quenching by Cl_2. The pseudo-first-order quenching plots for NF($a^1\Delta$) + Cl_2 at a variety of temperatures are shown in the upper panel. The resulting quenching rate constants are as follows: 300 K, $5.22 \pm 0.45 \times 10^{-13}$ cm^3 molecules^{-1} s^{-1}; 358 K, $6.60 \pm 0.34 \times 10^{-13}$ cm^3 molecules^{-1} s^{-1}; 393 K, $1.14 \pm 0.12 \times 10^{-12}$ cm^3 molecules^{-1} s^{-1}; 413 K, $1.29 \pm 0.14 \times 10^{-12}$ cm^3 molecules^{-1} s^{-1}; 473 K, $1.46 \pm 0.11 \times 10^{-12}$ cm^3 molecules^{-1} s^{-1}. The lower panel shows the Arrhenius plot for all measurements and gives $k(T) = 1.6 \pm 1.0 \times 10^{-11}$ exp(−1100 ± 250/T) cm^3 molecules^{-1} s^{-1} and $E_a = 2.2 \pm 0.5$ kcal mol^{-1}.

$$[NX(a^1\Delta)] = I(NX(a^1\Delta))^*\frac{\tau}{\text{response}} \qquad (12)$$

(τ(NCl) = 2, τ(NF) = 5 s, response(NF) = 0.8, and response-(NCl) = 0.2) is ∼ 0.45, compared with the efficiency[26] of Cl + N_3, ≥0.5.

Setser and Du measured room-temperature quenching of NF($a^1\Delta$) by Cl_2 and proposed chemical reaction as the dominant quenching mechanism, based on the unliklihood of a singlet−triplet curve crossing and the absence of product NF($X^3\Sigma^-$). The correlation diagram in the lower panel of Figure 3 is based on $\Delta H^0_f(NFCl)$[27] = 38.7 kcal mol^{-1}, D_0(NFCl−Cl)[18] = 52.7

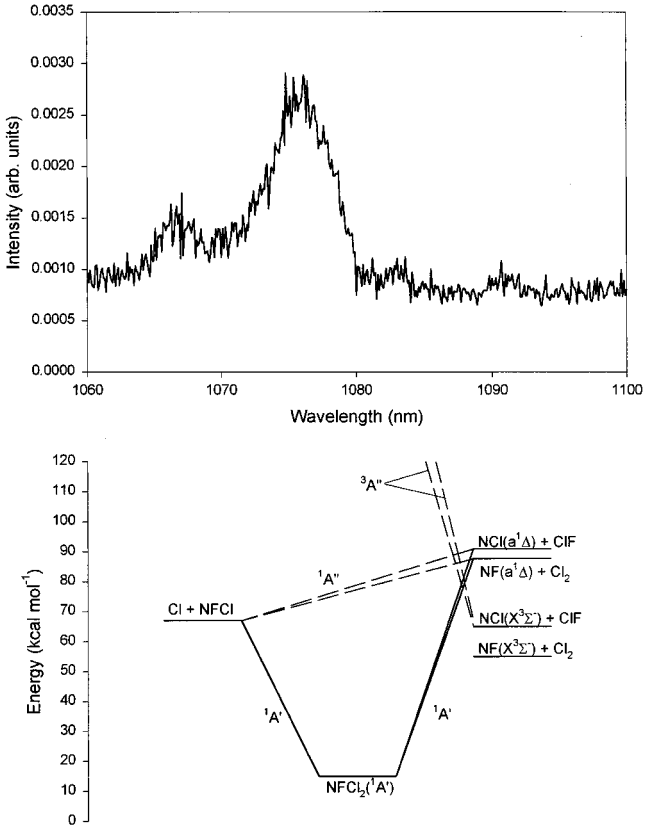

Figure 3. Products of NF($a^1\Delta$) + Cl_2. Upper panel: An NCl($a^1\Delta$) spectrum observed for $T = 413$ K, $[HN_3]_0 = 1.3 \times 10^{13}$, $[F]_0 = 7.7 \times 10^{12}$, and $[Cl_2]_0 = 2.5 \times 10^{13}$ cm^{-3}. At the point of Cl_2 injection ($\Delta t = 0.019$ s), $[F] \approx 0$, and $[HN_3] = 6.4 \times 10^{12}$. The NCl($a^1\Delta$) is probably produced by a chemical reaction between NF($a^1\Delta$) and Cl_2 to produce NFCl + Cl, followed by Cl + HN_3 and/or Cl + N_3, see text. Lower panel: A correlation diagram showing the possible quenching pathways for NF($a^1\Delta$) + Cl_2 is shown; see text for details.

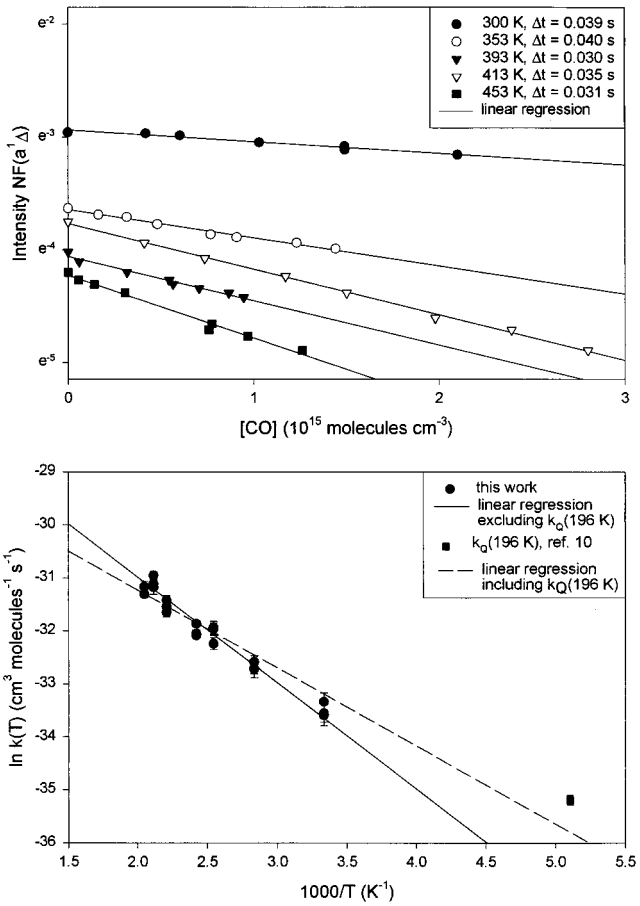

Figure 4. Temperature-dependent quenching by CO. The pseudo-first-order quenching plots for NF($a^1\Delta$) + CO at a variety of temperatures are shown in the upper panel. The resulting quenching rate constants are as follows: 300 K, $2.68 \pm 0.48 \times 10^{-15}$ cm^3 molecules^{-1} s^{-1}; 353 K, $6.23 \pm 0.65 \times 10^{-15}$ cm^3 molecules^{-1} s^{-1}; 393 K, $1.31 \pm 0.17 \times 10^{-14}$ cm^3 molecules^{-1} s^{-1}; 413 K, $1.16 \pm 0.04 \times 10^{-14}$ cm^3 molecules^{-1} s^{-1}; 453 K, $1.80 \pm 0.17 \times 10^{-14}$ cm^3 molecules^{-1} s^{-1}. The lower panel shows the Arrhenius plot for all measurements and shows two possible linear regression fits. The solid line excludes k_Q(196) and gives $k(T) = 2.0 \times 10^{-12}$ exp(−2020/T) and $E_a = 4.0$ kcal mol^{-1}. If k_Q(196) is included, the fit indicated by the broken line gives $k(T) = 6.5 \times 10^{-13}$ exp(−1470/T) and $E_a = 2.9$ kcal mol^{-1}.

kcal mol^{-1}, and $\Delta H_f^0(NCl)^{28} = 77$ kcal mol^{-1}. The intermediate species $NFCl_2(\tilde{X}, {}^1A')$ may eliminate a diatom of Cl_2 or ClF, leaving ground-state NF($X^3\Sigma^-$) or NCl($X^3\Sigma^-$), respectively. Alternatively, a Cl atom may be ejected to give NFCl. This latter product set is the most likely since ground-state NCl or NF formation requires a singlet−triplet curve crossing, and the NCl($a^1\Delta$) spectrum is consistent with the Cl + N_3 reaction. Further evidence could be obtained by detection of the NFCl radical, which has been isolated and detected in low-temperature argon matrixes.[27]

(ii) Quenching by CO: The room-temperature quenching rate constant[10,17] for CO + NF($a^1\Delta$) is small, $k(300\text{ K}) = 3.6 \pm 0.4 \times 10^{-15}$ cm^3 molecules^{-1} s^{-1}, and proceeds by chemical reaction to produce F + NCO($\tilde{X}^2\Pi$). Since NF($a^1\Delta$) + CO produces F atoms and our experiments were performed in the presence of excess HN_3 (and N_3), it is possible that NF($a^1\Delta$) could be regenerated. If significant, this process could lead to rate constant values that are dependent on the reaction time and underestimation of the true k_Q. At short Δt the cumulative effect of NF regeneration is inconsequential but increases steadily with increased reaction time. Fortunately, our k_Q measurements are invariant (within the experimental error) with Δt and are in excellent agreement with the room-temperature results of Du and Setser[10] where HN_3 was not in excess and NF($a^1\Delta$) could not be regenerated. Thus, we conclude that F atom regeneration via reaction 5a is not important for our conditions.

The rate constant increases slightly with increased temperature, qualitatively consistent with the trend observed by Du at 196 K[10] (see Figure 4). The Arrhenius plot in the lower panel of Figure 4 gives $k(T, \text{CO}) = 2.0 \times 10^{-12}$ exp(−2020/T) and $E_a = 4.0$ kcal mol^{-1} if Du's low-temperature measurement is excluded. If k_Q(196 K) is included in the fit, $k(T, \text{CO}) = 6.5 \times 10^{-13}$ exp(−1470/T) and $E_a = 2.9$ kcal mol^{-1}. The linear regression fit to our data is better without k_Q(196 K) and considering the difficulty in measuring such a small rate constant, it is possible that the result at 196 K is overestimated. We recommend $k(T, \text{CO}) = 2.0 \pm 1.0 \times 10^{-12}$ exp(−2000 ± 250/T) cm^3 molecules^{-1} s^{-1} and $E_a = 4.0 \pm 0.5$ kcal mol^{-1}.

(iii) Quenching by O_2: The quenching rate constant by molecular oxygen is small at room temperature ($k_Q(300\text{ K}) = 7.0 \pm 0.7 \times 10^{-15}$ cm^3 molecules^{-1} s^{-1}) and increases by less than a factor of 3 at 490 K. The upper panel of Figure 5 shows the results of several quenching experiments, while the lower panel gives the Arrhenius plot. Some early experiments were performed with a dilute mixture of O_2 in Ar. Unfortunately, these mixtures did not give much quenching of NF($a^1\Delta$) and the resulting rate constants have large scatter for repeated measurements. Subsequent experiments were performed with an O_2 lecture bottle directly attached to the metering valve, and the scatter for repeated measurements was much better. Hence,

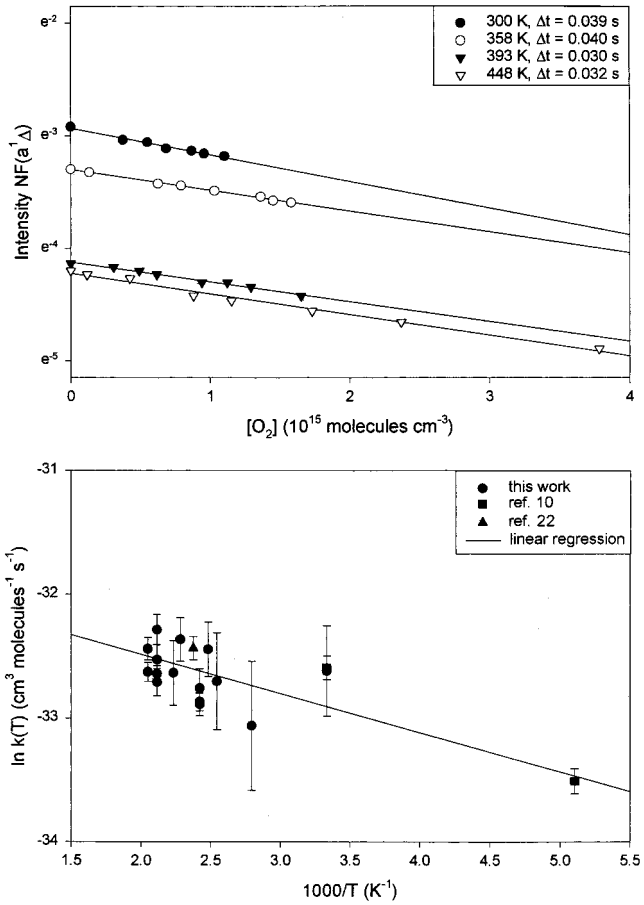

Figure 5. Temperature-dependent quenching by O_2. The pseudo-first-order quenching plots for $NF(a^1\Delta) + O_2$ at a variety of temperatures are shown in the upper panel. The resulting quenching rate constants are as follows: 300 K, $6.07 \pm 0.75 \times 10^{-15}$ cm^3 molecules^{-1} s^{-1}; 358 K, $4.63 \pm 0.23 \times 10^{-15}$ cm^3 molecules^{-1} s^{-1}; 393 K, $5.86 \pm 0.59 \times 10^{-15}$ cm^3 molecules^{-1} s^{-1}; 448 K, $5.72 \pm 0.53 \times 10^{-15}$ cm^3 molecules^{-1} s^{-1}. The lower panel shows the Arrhenius plot for all measurements and gives $k(T) = 1.5 \times 10^{-14}$ exp(−320/T) cm^3 molecules^{-1} s^{-1} and $E_a = 0.6$ kcal mol^{-1}.

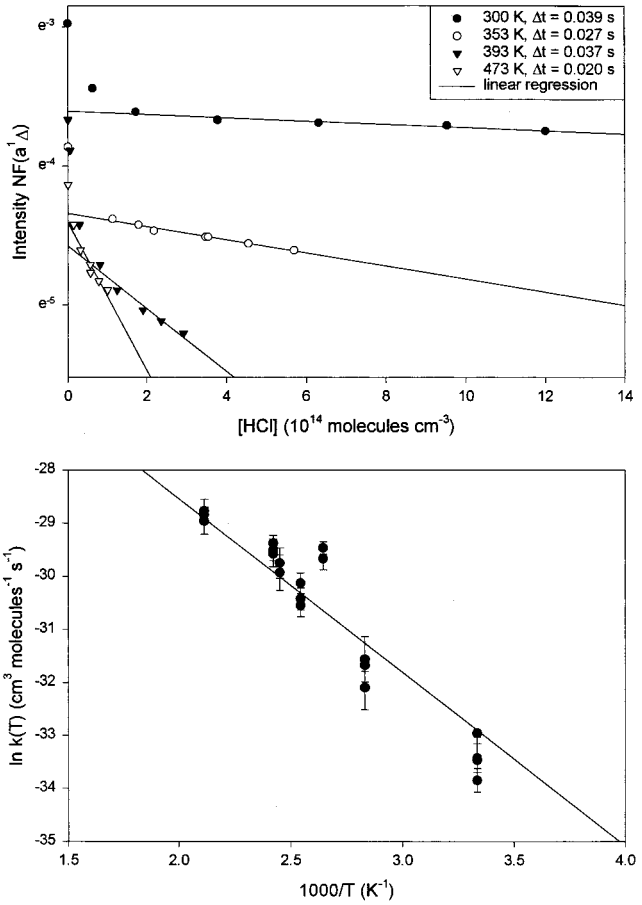

Figure 6. Temperature-dependent quenching by HCl. The pseudo-first-order quenching plots for $NF(a^1\Delta)$ + HCl at a variety of temperatures are shown in the upper panel. The resulting quenching rate constants are: 300 K, $3.04 \pm 0.94 \times 10^{-15}$ cm^3 molecules^{-1} s^{-1}; 353 K, $1.75 \pm 0.21 \times 10^{-14}$ cm^3 molecules^{-1} s^{-1}; 393 K, $6.09 \pm 1.40 \times 10^{-14}$ cm^3 molecules^{-1} s^{-1}; 473 K, $2.65 \pm 0.72 \times 10^{-13}$ cm^3 molecules^{-1} s^{-1}. Lower panel: The linear regression for the Arrhenius plot $k(T) = 2.8 \times 10^{-10}$ exp(−3270/T) cm^3 molecules^{-1} s^{-1} and $E_a = 6.5$ kcal mol^{-1}.

some of the data points on the upper panel of Figure 5 represent the average of three measurements at the same temperature and have much larger error bars. Even though the agreement with previous experiments is reasonable, the scatter on the Arrhenius plot shown in the lower panel of Figure 5 is significant. The best linear regression fit gives $k(T) = 1.5 \times 10^{-14}$ exp(−320/T) cm^3 molecules^{-1} s^{-1} and $E_a = 0.6$ kcal mol^{-1}. It is important to note, however, that if the 196 K data point is discarded, $k(T, O_2)$ is independent of temperature for the range shown. Indeed, Setser and Du[10] report $k_Q(300\ K) = 7.0 \pm 0.7 \times 10^{-15}$ cm^3 molecules^{-1} s^{-1} while Heidner et al.[22] recommend $k_Q(421\ K) = 8.2 \pm 0.8 \times 10^{-15}$ cm^3 molecules^{-1} s^{-1}; these values are identical within the combined error bars. Providing that the data point at 196 K is accurate and assuming 50% uncertainty for the activation energy, we recommend $k(T) = 1.5 \pm 0.5 \times 10^{-14}$ exp(−300 ± 150/T) cm^3 molecules^{-1} s^{-1} and $E_a = 0.6 \pm 0.3$ kcal mol^{-1}. The small temperature dependence is consistent with an energy transfer reaction.

(iv) Quenching by HCl: The room-temperature quenching rate constant for HCl is small, $k_Q = 1.6 \pm 0.3 \times 10^{-15}$ cm^3 molecules^{-1} s^{-1}, and our result, $3.6 \pm 2.2 \times 10^{-15}$ cm^3 molecules^{-1} s^{-1}, is in reasonable agreement with Du's value. As previously mentioned for Cl_2 quenching, the $NF(a^1\Delta)$ signal dropped sharply upon addition of a small [HCl]. Further addition of HCl resulted in slower quenching, and linear plots were obtained (see Figure 6). However, the reaction rate increases dramatically with temperature. At 450 K, $k_Q \cong 1.0 \times 10^{-12}$ cm^3 molecules^{-1} s^{-1}, nearly 3 orders of magnitude larger. The linear regression for the Arrhenius plot in the lower panel gives $E_a = 6.5$ kcal mol^{-1}, and a gas-kinetic value for the pre-exponential factor, $A = 2.8 \times 10^{-10}$ cm^3 molecules^{-1} s^{-1}. The potential complication of HCl + F reactions which would remove F atoms and prevent reaction 1 was avoided by running the experiment with excess HN_3.

The large pre-exponential factor requires special defense, especially considering the high uncertainty of replicate measurements at the same temperature. The most obvious potential source of error is reagent impurity. However, the HCl should have been pure since a new bottle of semiconductor grade HCl (99.999%) was used to prepare the HCl samples, and in all cases at least one gas phase distillation (where the only the middle third was retained) was performed to eliminate any possible H_2/Cl_2 impurity. Another possibility is a stoichiometry factor that is greater than unity. For example, if any of the products of the initial quenching reaction (NFCl, HNF, HNFCl, Cl, or HF) efficiently quenched $NF(a^1\Delta)$, then the total quenching rate constant would be equal to the rate constant for the rate-determining step multiplied by the total number of $NF(a^1\Delta)$ molecules removed by all subsequent reactions. Considering the $NF(a^1\Delta) + Cl_2$ reaction as a model for insertion reactions, a

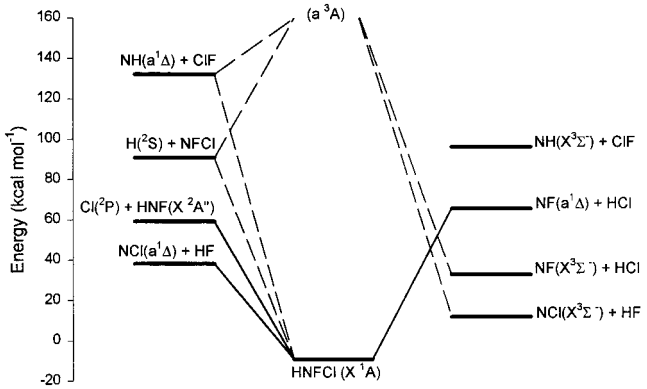

Figure 7. Products of NF($a^1\Delta$) + HCl. A correlation diagram showing the thermochemistry and possible quenching pathways for NF($a^1\Delta$) + HCl is shown; see text for details.

pre-exponential factor of $\sim(2-5) \times 10^{-11}$ may be expected, and the stoichiometry factor needs to be 6−10. However, since Cl, F, HF, etc. are all known to be inefficient quenchers of NF($a^1\Delta$), only HNF, if present in sufficient quantities, could quench NF($a^1\Delta$) and contribute to a larger stoichiometry factor. A third possibility involves physical quenching by a nonadiabatic curve crossing to NF($X^3\Sigma^-$) + HCl which could, in principle, lead to unusual temperature dependencies. In light of these arguments and the quality of the data, we recommend $k(T) = 2.0 \pm 1.0 \times 10^{-10}$ exp(−3270 ± 250/T) cm^3 molecules^{-1} s^{-1} and $E_a = 6.5 \pm 0.5$ kcal mol^{-1} as an upper limit.

An NCl($a^1\Delta$) spectrum was observed for HCl quenching of NF($a^1\Delta$). The NCl($a^1\Delta$) spectrum produced by HCl quenching is slightly lower in intensity compared to the one described above for quenching by Cl_2. The source of this NCl($a^1\Delta$) spectrum requires some comment. The lower panel of Figure 7 shows a schematic representation of the HCl + NF($a^1\Delta$) reaction channels. The diagram is based on D_0(H−NFCl)[18] ≥ 100, $\Delta H_f^0(HNF)$[29] = 30.4, $\Delta H_f^0(NFCl)$[27] = 38.7, and $\Delta H_f^0(NH)$[30] = 84.2 kcal mol^{-1}. If D_0(H−NFCl) = 100 is assumed, D_0(Cl−HNF) = 68.5 kcal mol^{-1}, which is slightly larger than the dissociation energies of similar species: D_0(Cl−NFCl)[18] = 52.7, D_0(CF_3NCl−Cl)[31] ≤ 56, D_0(CF_2ClNCl−Cl)[31] ≤ 57 and D_0(CF_2N−Cl)[31] ≤ 56 kcal mol^{-1}. H atom elimination and NH + ClF formation from HNFCl are precluded due to energetic constraints in our experiment. On the other hand, quenching of NF($a^1\Delta$) to make HNFCl($\tilde{X}$ ^{1}A) may lead to NCl($a^1\Delta$) + HF(v ≤ 2) or HNF(X ^{2}A″) + Cl(^{2}P). In the latter case, the Cl atom could react with residual HN_3 or N_3 to give rise to the observed NCl($a^1\Delta$). The important question then is whether Cl rupture from Cl−HNF can compete with HF elimination considering that $\Delta H_f^0(Cl + HNF)$ is 21 kcal mol^{-1} larger than $\Delta H_f^0(HF + NCl(a^1\Delta))$. As was the case for NF($a^1\Delta$) + Cl_2, the intensity of the NCl($a^1\Delta$) spectrum is consistent with the branching fraction of the Cl + N_3 reaction.[26] The conversion efficiency, calculated by eq 11 is ∼0.65, slightly larger than the efficiency[26] of Cl + N_3. In light of the fact that barriers for diatomic elimination are typically higher than those of atomic elimination, the generation of Cl + HNF is not impossible. However, the estimated height of the barrier for reaction 9c (based on the measured value of the rate constant for the reverse reaction,[16] k(300 K) = 5 ± 3 × 10^{-15} cm^3 molecules^{-1} s^{-1}) is ≤54 kcal mol^{-1}, and reaction 9e is still the thermodynamically preferred product channel.

Examination of other reactions that produce the same intermediate provides some useful information. The Coombe laboratory has reported NCl($a^1\Delta$) production following quenching of NH($a^1\Delta$) by ClF[19] (which probes the same intermediate as the present results) and Cl_2 (which is related to the H + NCl_3 reaction).[32] However, in both cases, they believed that NCl($a^1\Delta$) was formed directly rather than via secondary reactions with HNCl. The HNFCl intermediate formed by the H + NFCl reaction has been examined by the Setser[18] and Coombe[20] laboratories. Both groups found that the NF($a^1\Delta$) formation channel is more important than the NCl($a^1\Delta$) formation channel, even though NCl($a^1\Delta$) is the energetically favored product. Two important differences between the present results and the H + NFCl experiments should be noted. First, because we generate HNFCl by HCl + NF($a^1\Delta$), the intermediate species has considerably less internal energy than when it is generated via H + NFCl. In addition, it is important to note that both H + NFCl experiments used excess H atoms, and even though Cl + HNF may be a viable reaction pathway, H + HNF reactions do not generate NF($a^1\Delta$) because this reaction is at best, thermoneutral.

$$H + HNF \rightarrow H_2 + NF(a^1\Delta) \qquad \Delta H_r^0 = 5.3 \text{ kcal mol}^{-1} \tag{13a}$$

$$\rightarrow HF + NH(a^1\Delta) \qquad \Delta H_r^0 = -32.3 \text{ kcal mol}^{-1} \tag{13b}$$

Unfortunately, the present results only to add to the mystery—is there a third (Cl + HNF) channel for H + NFCl? If so, what is the branching fraction relative to HCl + NF($a^1\Delta$) and HF + NCl($a^1\Delta$) and what is the total H atom removal rate constant? If not, why is the least exothermic channel so dominant? Clearly, there is much that remains to be understood about the unimolecular decomposition of chemically activated HNFCl.

Conclusions

The temperature dependence of 4 NF($a^1\Delta$) quenching reactions have been measured in a fast flow reactor. The rate constant data were fit by Arrhenius expressions $k(T, Cl_2) = 1.6 \pm 1.0 \times 10^{-11}$ exp(−1100 ± 250/T), $k(T, CO) = 2.0 \pm 1.0 \times 10^{-12}$ exp(−2000 ± 250/T), $k(T, HCl) = 2.0 \pm 1.0 \times 10^{-10}$ exp(−3270 ± 250/T), and $k(T, O_2) = 1.5 \pm 0.5 \times 10^{-14}$ exp(−300 ± 150/T) cm^3 molecules^{-1} s^{-1}. Chemical reaction is the mechanism for quenching by CO, Cl_2, and HCl and product NCl($a^1\Delta$) was observed for the latter two molecules. In both cases, we believe that some of the quenching reactions produce Cl atoms that react with residual HN_3 and/or N_3. Our proposed mechanisms can be tested by LIF detection of HNF or NFCl.[33,34]

The present results have importance for the isovalent NCl($a^1\Delta$) molecule. In general, most NCl($a^1\Delta$) quenching rate constants[16] are slightly smaller or comparable to those of NF($a^1\Delta$), although Q = O_2 and HCl are notable exceptions (k_{NCl}(300 K, O_2) = 2.8 ± 0.6 × 10^{-12} and k_{NCl}(300 K, HCl) = 1.5 ± 0.4 × 10^{-14} cm^3 molecules^{-1} s^{-1}). The temperature dependence of NCl($a^1\Delta$) quenching reactions should be very similar to NF($a^1\Delta$).

Acknowledgment. The U.S. Air Force Office of Scientific Research supported this work. G.C.M also acknowledges the National Research Council for support. The authors are grateful for helpful discussions with Profs. R. D. Coombe, M. C. Heaven, and D. W. Setser.

References and Notes

(1) Benard, D. J.; McDermott, W. E.; Pchelkin, N. R.; Bousek, R. R. *Appl. Phys. Lett.* **1979**, *34*, 40, and references therein.

(2) Wayne, R. P. Reactions of Singlet Molecular Oxygen in the Gas Phase. In *Singlet Oxygen*; Frimer, A. A., Ed.; CRC Press: Boca Raton, FL, 1985.
(3) Hack, W.; Wilms, A. *J. Phys. Chem*. **1989**, *93*, 3540.
(4) Hack, W.; Rathmann, K. *J. Phys. Chem*. **1992**, *96*, 47.
(5) Hack, W.; Wagner, H. G.; Zasypkin, A. *Ber. Bunsen-Ges. Phys. Chem.*, **1994**, *98*, 156.
(6) Adams, J. S.; Pasternack, L. *J. Phys. Chem*. **1991**, *95*, 2975.
(7) Freitag, F.; Rohrer, F.; Stuhl, F. *J. Phys. Chem*. **1989**, *93*, 3170.
(8) Hack, W.; Jordan, R. *Ber. Bunsen-Ges., Phys. Chem*. **1997**, *101*, 545.
(9) Quinones, E.; Habdas, J.; Setser, D. W. *J. Phys. Chem*. **1987**, *91*, 5155.
(10) Du, K. Y.; Setser, D. W. *J. Phys. Chem*. **1990**, *94*, 2425.
(11) Du, K. Y.; Setser, D. W. *J. Phys. Chem*. **1992**, *96*, 2553.
(12) Du, K. Y.; Setser, D. W. *J. Phys. Chem*. **1991**, *95*, 4728.
(13) Du, K. Y.; Setser, D. W. *J. Phys. Chem*. **1993**, *97*, 5266.
(14) Davis, S. J.; Rawlins, W. T.; Piper, L. G. *J. Phys. Chem*. **1989**, *93*, 1078.
(15) Hewett, K. B.; Setser, D. W. *Chem. Phys. Lett*. **1998**, *297*, 335.
(16) Hewett, K. B.; Manke, G. C., II; Setser, D. W.; Brewood, G. *J. Phys. Chem. A*, in press.
(17) Wategaonkar, S.; Du, K. Y.; Setser, D. W. *Chem. Phys. Lett*. **1992**, *189*, 586.
(18) Arunan, E.; Liu, C. P.; Setser, D. W.; Gilbert, J. V.; Coombe, R. D. *J. Phys. Chem*. **1994**, *98*, 494.
(19) Singleton, S. M.; Coombe, R. D. *J. Phys. Chem*. **1995**, *99*, 16296.
(20) Exton, D. B.; Gilbert, J. V.; Coombe, R. D. *J. Phys. Chem*. **1991**, *95*, 7758.
(21) Herbelin, J. M. Private communication.
(22) Weiller, B. H.; Heidner, R. F.; Holloway, J. S.; Koffend, J. B. *J. Phys. Chem*. **1992**, *96*, 9321.
(23) Henshaw, T. L.; Herrerra, S. D.; Schlie, L. A. *J. Phys., Chem. A* **1997**, *102*, 4048.
(24) Kolts, J. H.; Setser, D. W. In *Reactive Intermediates in the Gas Phase*; Setser, D. W., Ed.; Academic Press: New York, 1979.
(25) Coombe, R. D. Private communication.
(26) Manke, G. C., II; Setser, D. W. *J. Phys. Chem. A* **1998**, *102*, 7257.
(27) Gilbert, J. V.; Okin, G. S. *J. Phys. Chem*. **1995**, *99*, 11365.
(28) Xantheas, S. S.; Dunning Jr., T. H.; Mavidis, A. *J. Chem. Phys*. **1997**, *106*, 3280.
(29) Sana, M.; Leroy, G.; Peeters, D.; Younang, E. *J. Mol. Struct*. **1987**, *151*, 325.
(30) *CRC Handbook of Chemistry and Physics*, 71st ed.; Lide, D. R., Ed., CRC Press: Boca Raton, FL.
(31) Zhang, F. M.; Oba, D.; Setser, D. W. *J. Phys. Chem*. **1987**, *91*, 1099.
(32) Singleton, S. M.; Coombe, R. D. *Chem. Phys. Lett*. **1993**, *215*, 237.
(33) Chen, J.; Dagdigian, P. J. *J. Chem. Phys*. **1992**, *96*, 7333.
(34) Hewett, K. B., Setser, D. W. *J. Phys. Chem. A* **1997**, *101*, 9125.